

## Free-induction decay after saturation in dilute ruby

R. Boscaino

*Dipartimento di Scienze Fisiche, Università di Cagliari, Cagliari, Italy*

F. M. Gelardi

*Istituto di Fisica, Via Archirafi 36, I 90123 Palermo, Italy*

(Received 20 June 1991)

The after-saturation free-induction-decay (FID) rate of an electron spin transition has been measured in a dilute ruby sample, and a marked departure from the Bloch-like behavior has been found. The similarity with the results obtained recently by Szabo and Muramoto [Phys. Rev. A **39**, 3992 (1989)] in the same system but for optical FID points out the close link between the non-Bloch behavior of the FID emission observed in optics and in magnetic-resonance systems. Our results are compared with the theoretical predictions of a statistical theory of the FID emission, but poor agreement is found.

PACS number(s): 42.50.Md, 42.65.Ky, 76.30. - v

Free-induction decay (FID) in impurity-ion solids has been the subject of much theoretical and experimental work in recent years. A reason is that FID experiments have been used to demonstrate the restricted validity of the phenomenological Bloch equations to describe the saturated state of a system of two-level centers in a solid matrix.

Experimental evidence of the failure of the optical Bloch equations to account for the properties of the FID emission in solids was reported first by De Voe and Brewer [1] for the  $^1D_2$  line of  $\text{Pr}^{3+}:\text{LaF}_2$  and, more recently, by Szabo and Muramoto [2] in  $\text{Cr}^{3+}:\text{Al}_2\text{O}_3$ . Major departures from the predictions of the Bloch equations were found in both cases as regards the order of magnitude of the decay rate  $\Gamma$  of the FID signal (much slower than expected) and especially its dependence on the intensity of the saturating electromagnetic (e.m.) field.

The anomalous (non-Bloch) behavior of the FID rate in solid systems is generally ascribed to the fluctuations of the resonance frequencies of the individual active centers, randomly perturbed by the host environment. Several statistical theories [3–9] of the FID emission have calculated, for a wide variety of noise models, that the resonance-frequency noise reduces the power broadening of the hole burnt within the inhomogeneous line with respect to a purely static inhomogeneous broadening, thus causing a longer persistence of the FID emission. This is in qualitative agreement with the lengthening of the FID decay time observed experimentally. However, the validity of the theoretical treatments developed till now, and especially the specific stochastic model to be used to model the frequency noise, are a matter of current debate.

The non-Bloch behavior of the FID signal is not peculiar of optical transitions and it has been observed as well in magnetic resonance systems [10,11]. In a recent paper [11] we reported an extensive experimental study on the FID regime in magnetic resonance solid systems ( $E'$  centers in silica,  $[\text{AlO}_4]^\ominus$  centers in quartz), where we

measured anomalies of the FID rate that closely resemble those observed in optical transitions. In magnetic resonance experiments these anomalies could be observed for a much wider range of the field intensity than in optical ones and, by using nonlinear-spectroscopy techniques, data scattering was kept lower. Taking advantage of these peculiarities, we could carry out a reliable comparison with the results of the statistical theories and we showed that, at least in those systems, the statistical theories could not account for the qualitative features of the power dependence of the FID rate.

In this Brief Report we wish to complete our previous paper by reporting further measurements on the power dependence of the FID rate as obtained in a magnetic resonance line of  $\text{Cr}^{3+}:\text{Al}_2\text{O}_3$ , namely, the same active center in the same host matrix as used in Ref. [2] for optical FID experiments. The comparison between the results reported here and those of Ref. [2] points out the close link between the non-Bloch behavior observed in optical and electron spin transitions. In this regard it is worth noting that in dilute ruby the dephasing mechanisms of both transitions are of magnetic dipolar origin [8,12]. Moreover, in our opinion, a further reason of interest of the results reported here is that they make apparent, perhaps more than previous results, that the statistical theories of the FID emission fail to give a quantitative account of the experimental data, even in the high power limit.

As a general scheme, a FID experiment consists of a preparative stage and of a monitoring one. During the former the system is preliminarily prepared in a saturated steady state by a long pulse  $(-t_0, 0)$  of resonant radiation whose intensity is usually given in terms of the induced Rabi frequency  $\chi$ . In the latter  $(t > 0)$ , FID emission occurs as caused by the coherences established within the system at  $t < 0$  and that survive the trailing edge of the driving field pulse. In particular, for a highly inhomogeneous resonance line, having a width  $\sigma$ , the FID signal consists of a fast growth from the steady-state response

toward a maximum at very short times ( $t \ll \sigma^{-1}$ ), followed by a slower decay at longer times ( $t \gg \sigma^{-1}$ ). Here we are concerned with the decay part, usually described as a single exponential decay with a rate  $\Gamma$ .

The experimental apparatus and procedure used for the measurements reported below are essentially the same as reported in our previous paper [11] and will not be repeated here. Here we limit ourselves to recall that in our experimental setup the saturation of the resonance line is accomplished by means of two-photon (TP) transitions: during the preparative stage, the spin system, tuned to  $\omega_0$  by the static field  $\mathbf{B}_0$ , is driven by a microwave field  $\mathbf{b}_1$  polarized at an angle  $\alpha = 45^\circ$  with respect to the static field and oscillating at frequency  $\omega_1 = \omega_0/2$ . This configuration is often referred to as TP-excited second-harmonic (SH) FID, as the system is prepared by a TP-resonant field and the FID emission occurs in an e.m. band centered at the SH frequency of the input field. Its advantages stem from the large spectral distance between the exciting field ( $\omega_1$ ) and the system emission ( $\omega_0 = 2\omega_1$ ), which saves the small FID signal from being buried under the trailing edge of the much more intense input field. From an experimental point of view, this property is crucial for the system investigated here, where the FID signal decays to the noise level in a few  $\mu\text{s}$ . From a conceptual point of view, exciting the FID emission by means of TP transitions is of little consequence. In fact, as shown previously [11], all the expressions calculated for the standard one-photon-excited FID emission apply as well to the TP-excitation case provided that the Rabi frequency  $\chi$  is given the meaning of the TP-Rabi frequency  $\chi_{\text{TP}}$  [13]:

$$\chi_{\text{TP}} = \frac{1}{2\omega} (V_{ii} - V_{jj}) V_{ij}, \quad (1)$$

where  $V_{ij}$  ( $i, j = 1, 2$ ) are the matrix elements of the interaction  $V = -\gamma \mathbf{b}_1 \cdot \mathbf{S}$  with the input field between the states  $|i\rangle$  and  $|j\rangle$  involved in the transition and  $\gamma$  is the gyromagnetic ratio.

The measurements reported here were taken in a sample of  $\text{Cr}^{3+}:\text{Al}_2\text{O}_3$  with nominal concentration 0.009 wt %  $\text{Cr}_2\text{O}_3$ , at  $T = 4.2$  K and with the static field  $\mathbf{B}_0$  perpendicular to the  $c$  crystal axis, at the high-field resonance line, usually indicated as  $|-\frac{3}{2}\rangle \leftrightarrow |-\frac{1}{2}\rangle$  resonance [14]. This line is centered at  $B_0 = 0.395$  T at our working frequency  $\omega_0 = (2\pi)5.9$  GHz and is inhomogeneously broadened by the superhyperfine interaction of the electron spin of the  $\text{Cr}^{3+}$  with the nuclear spins of the neighboring  $^{27}\text{Al}$  ions. The resonance line has a Gaussian shape with a width  $\Delta B = 0.65$  mT, corresponding to  $\sigma = (2\pi)18$  MHz. In the same experimental conditions as for FID experiments, we measured the following values of the relaxation times in our sample:  $T_1 = 95 \pm 15$  ms,  $T_2 = 7.5 \pm 0.7$   $\mu\text{s}$ .  $T_2$  was measured by spin-echo experiments and  $T_1$  by the saturation recovery method. The value of  $T_1$  is to be considered as indicative of the order of magnitude as the experimentally observed recovery was not exponential.

By using literature data [14] for the composition of the states  $|-\frac{3}{2}\rangle$  and  $|-\frac{1}{2}\rangle$  of the  $\text{Cr}^{3+}$  ion in ruby for  $\mathbf{B}_0 \perp \mathbf{c}$

and  $B_0 = 0.395$  T, we get the following expression of  $\chi_{\text{TP}}$ :

$$\chi_{\text{TP}} = 0.48\gamma^2 b_1^2 / \omega_0 \quad (2)$$

in terms of the amplitude  $b_1$  of the microwave field at frequency  $\omega_1$  acting on the sample. The labels TP will be dropped hereafter.

Experimental data are reported in Fig. 1, where the measured values of the FID rate  $\Gamma$  are plotted versus the Rabi frequency  $\chi$ , both in frequency units. At each value of the input power,  $\chi$  was determined by inserting the appropriate value of  $b_1$  into Eq. (2);  $b_1$  was in turn determined by a preliminary calibration based on the detection of the nutational wiggles of a reference sample ( $E'$  centers in silica). This indirect determination of  $\chi$  was necessary since the decay of the nutational regime in dilute ruby was too fast to allow a reliable direct measurement of  $\chi$ . At each value of  $\chi$ , the rate  $\Gamma$  was measured by fitting the time-dependent amplitude of the FID signal  $S(t)$  to a single exponential law:  $S(t) = C \exp(-\Gamma t)$ .

The explored window of  $\chi$  ranges from 50 to 500 kHz. The lower limit was fixed by signal-to-noise ratio conditions. On the high- $\chi$  side, the upper limit was fixed by the bandwidth of the cavity mode, which makes unreliable the measurements of rates faster than 750 kHz.

Two theoretical curves are also reported in Fig. 1. The curve labeled as  $B$  plots the theoretical power dependence of the FID rate  $\Gamma_B$  as obtained by solving the standard phenomenological Bloch equations for the FID emission in a highly inhomogeneous system [1]:

$$\Gamma_B = (1/T_2) [1 + (1 + \chi^2 T_1 T_2)^{1/2}]. \quad (3)$$

We recall that the approximations  $\chi \ll \sigma$  and  $\sigma T_2 \gg 1$

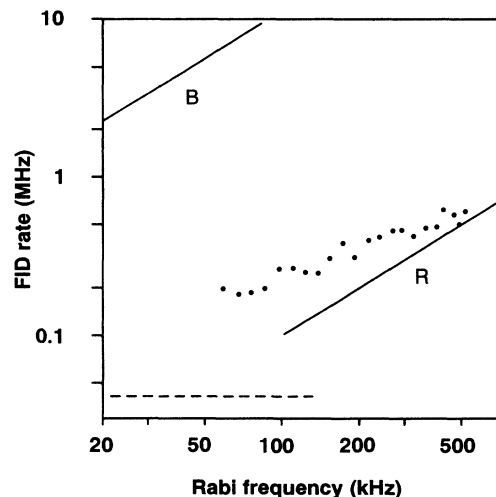


FIG. 1. Experimental dependence of the FID rate  $\Gamma/2\pi$  on the Rabi frequency  $\chi/2\pi$  in our sample of dilute ruby, for  $\mathbf{B}_0$  perpendicular to the  $c$  axis and  $B_0 = 0.395$  T. The full lines marked  $B$  and  $R$  plot the theoretical dependence expected from the Bloch and Redfield theory, respectively. The dashed line marks the low-power limit  $\Gamma_B(\chi=0)$  of the Bloch curve:  $\Gamma_B(\chi=0) = 2/T_2 = (2\pi)42.4$  kHz.

are to be used to get Eq. (3) [11]; both are well satisfied in our experimental conditions where  $\sigma T_2 = 0.85 \times 10^3$ ,  $\chi/\sigma \leq 0.03$ . The dashed line in Fig. 1 points out the low-power limit  $\Gamma_B(\chi=0) = 2/T_2$  of Eq. (3).

Curve *R* in Fig. 1 represents the asymptotic high-power limit of  $\Gamma(\chi)$ , as obtained from the Redfield theory [15]:  $\Gamma_R = \chi$ . According to this thermodynamic theory, the phase relaxation is slowed in the presence of a strong resonant field and the transverse relaxation time  $T_2$  has to be replaced by a power-dependent effective time  $T_{2e}$  with limiting values  $T_2$  (low power) and either  $T_1$  (open systems) or  $2 T_1$  (closed systems) for  $\chi \rightarrow \infty$ . This limit was derived by Redfield on the basis of thermodynamics considerations, but it is as well obtained as a limit by all the statistical theories [3–9] of FID emission. The curve  $\Gamma_R = \chi$  plotted in Fig. 1 is the asymptotic behavior for  $\chi^2 T_1 T_2 \gg 1$  of the Bloch solution  $\Gamma_B$  [Eq. (3)] with  $T_2$  replaced by  $T_1$ .

The experimental results reported in Fig. 1 indicate clearly the extent to which the FID behavior in the magnetic resonance of our dilute ruby sample departs from the Bloch-like behavior and tends to the Redfield limit. Note that the distance of the experimental values of  $\Gamma$  from the Bloch curve amounts to nearly 2 orders of magnitude on the high- $\chi$  side.

To make easier the comparison between microwave and optical FID experiments, in Fig. 2 our experimental data are redrawn in the more conventional plot of the saturated linewidth  $\gamma = \Gamma - 1/T_2$  of the burnt hole versus  $\chi$ . The comparison of our Fig. 2 with Fig. 4 of Ref. [2] points out the close similarity between optical and magnetic resonance FID anomalies. In Table I we summarize the values and the ranges of the relevant parameters ( $T_1 T_2$ ,  $\chi T_2$ ,  $\chi^2 T_1 T_2$ , and  $\gamma$ ) in our experiments and in the optical ones [2]. The main difference is that the  $\chi$

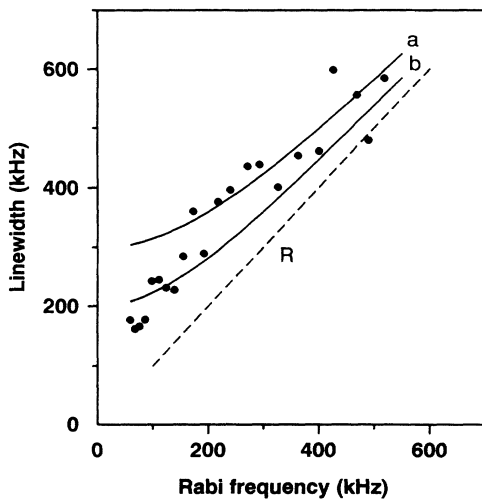


FIG. 2. Experimental values of the saturated linewidth  $\gamma/2\pi$  as a function of the Rabi frequency  $\chi/2\pi$ . The full lines plot the theoretical dependence of  $\chi$  as calculated from the Gaussian-Markov statistical theory, for  $\tau_c = 60 \mu\text{s}$  (a) and  $\tau_c = 90 \mu\text{s}$  (b).

TABLE I. Relevant parameters in optical and magnetic resonance FID experiments.

Quantity	Optical (Ref. [2])	Magnetic resonance (this work)
$(T_1 T_2)^{1/2}$ ( $10^{-4}$ s)	2.5	8.4
$\chi/2\pi$ (kHz)	8.5–85	50–500
$\chi^2 T_1 T_2$	$(0.2-20) \times 10^3$	$(0.7-70) \times 10^5$
$\chi T_2$	0.8–8	2.3–23
$\gamma/2\pi$ (kHz)	15–40	170–600

window explored here is shifted toward the high side. So, different parts of the transition from the Bloch limit toward the Redfield one are visible in the optical and microwave cases. In fact, as discussed in Ref. [11], this transition is controlled by the quantities  $\chi^2 T_1 T_2$  and  $\chi T_2$ . So, the tendency of the experimental FID rate to recover the Bloch behavior is more evident in the optical case, where smaller values of the saturation parameter can be explored. On the other hand, the magnetic resonance data better attain the Redfield limit as  $\chi T_2$  reaches higher values. However, even in the microwave case, the distance of the high-power data from the Redfield limit is still appreciable, as evident in Fig. 1.

Finally, we point out that the results reported here were obtained for a perpendicular orientation of  $\mathbf{B}_0$ , whereas the optical experiments were carried out for a parallel one. Our choice was motivated by signal-to-noise considerations and by the fact that the decay of the FID signal of magnetic resonance for  $\mathbf{B}_0 \parallel \mathbf{c}$  is too fast to allow us to explore in a reliable way the power dependence of  $\Gamma$  over a reasonable range of  $\chi$ . We remark that it would be of interest to carry out optical FID experiments also for a perpendicular orientation, in view of the different dynamics of the nuclear spins surrounding the  $\text{Cr}^{3+}$  in the two orientations [16].

Now we compare the experimental results reported here with the theoretical power dependence of the FID rate calculated by Yamanoi and Eberly [3]. In this theory the fluctuation  $\delta\omega(t)$  of the resonance frequency of the generic active center is modeled by an Ornstein-Uhlenbeck process, characterized by a mean square value  $\delta$  and a correlation time  $\tau_c$ . There is no *a priori* reason for preferring this Gaussian-Markov model to others and we chose it for the sake of simplicity as it yields a relatively simple approximate expression of  $\gamma$ :

$$\gamma = (\beta^2 + \chi^2 \beta T_1)^{1/2}, \quad (4a)$$

where

$$\beta = \frac{1}{T_2} \frac{\delta^2 \tau_c}{1 + \chi^2 \tau_c^2} + \frac{1}{T_1}. \quad (4b)$$

In Fig. 2 the experimental results are compared with the theoretical power dependence calculated from Eqs. (4) using the experimental values of  $T_1$  and  $T_2$ . If the condition

$$\frac{1}{T_2} = \frac{1}{T_1} + \delta^2 \tau_c \quad (5)$$

is imposed,  $\tau_c$  remains the only adjustable parameter. As shown in Fig. 2 the experimental points are enclosed by the theoretical curves obtained for  $\tau_c = 60 \mu\text{s}$  (a) and  $\tau_c = 90 \mu\text{s}$  (b), so they seem to be consistent with  $\tau_c = 75 \pm 15 \mu\text{s}$ . It is suggestive that this value is of the same order of the flipping time of the bulk nuclear spins of  $\text{Al}^{27}$  nuclei surrounding the electron spin [17]. However, this is no more than a mere coincidence, since so long a value of  $\tau_c$  apparently breaks the validity of the solution given in Eq. (4). In fact, according to Eq. (4b), this value of  $\tau_c$  implies  $\delta\tau_c = 3.3$ , which violates the condition  $\delta\tau_c < 1$  used to derive Eq. (4). On the other hand, if the value  $\tau_c = 7.5 \mu\text{s}$ , which is a limit for the validity of Eq. (4), is assumed, the corresponding theoretical curve falls out of scale of

Fig. 2 on the high- $\gamma$  side. This kind of discrepancy, which holds as well for optical FID data [2], is not a novelty, since it is met whenever the experimental data [1,2,10,11] on the power dependence of the saturated linewidth are compared with the theoretical results obtained by the statistical theories, independently of the specific model used to describe the frequency fluctuations. The need of alternative interpretations of the anomalous FID effect has often been claimed and several possibilities have been suggested but not yet put into complete theoretical treatments.

Helpful and stimulating discussions with A. Szabo and A. I. Burshtein are acknowledged with pleasure. The authors wish to thank G. Lapis and M. Quartararo for their technical assistance. This work has been supported by Ministero Universita e Ricerca, Roma, Italy (national and local funds).

- 
- [1] R. G. De Voe and R. G. Brewer, *Phys. Rev. Lett.* **50**, 1269 (1983).
- [2] A. Szabo and T. Muramoto, *Phys. Rev. A* **39**, 3992 (1989).
- [3] M. Yamanoi and J. H. Eberly, *J. Opt. Soc. Am. B* **1**, 751 (1984).
- [4] P. R. Berman and R. G. Brewer, *Phys. Rev. A* **32**, 2784 (1985).
- [5] P. R. Berman, *J. Opt. Soc. Am. B* **3**, 564 (1986); **3**, 572 (1986).
- [6] H. Tsunetsugu and E. Hanamura, *J. Phys. Soc. Jpn.* **55**, 3636 (1986).
- [7] A. I. Burshtein, A. A. Zharikov, and V. S. Malinovskii, *Zh. Eksp. Teor. Fiz.* **96**, 2061 (1989) [*Sov. Phys. JETP* **69**, 1164 (1989)]; *Phys. Rev. A* **43**, 1538 (1991).
- [8] S. Ya. Kilin and A. P. Nizovtsev, *Phys. Rev. A* **42**, 4403 (1990).
- [9] R. N. Shakhmuratov, *Pis'ma Zh. Eksp. Teor. Fiz.* **51**, 454 (1990) [*JETP Lett.* **51**, 514 (1990)].
- [10] R. Boscaino, F. M. Gelardi, and G. Messina, *Phys. Rev. A* **28**, 495 (1983).
- [11] R. Boscaino and V. M. LaBella, *Phys. Rev. A* **41**, 5171 (1990).
- [12] A. Szabo, T. Muramoto, and R. Kaarli, *Phys. Rev. B* **42**, 7769 (1990); A. Szabo and R. Kaarli, *ibid.* **44**, 12 307 (1991).
- [13] P. W. Milonni and J. H. Eberly, *J. Chem. Phys.* **68**, 1602 (1978); R. Boscaino and G. Messina, *Physica C* **138**, 179 (1986).
- [14] E. O. Schulz-du Bois, *Bell Syst. Tech. J.* **38**, 271 (1959); in *The Solid State Maser*, edited by J. W. Orton *et al.* (Pergamon, Oxford, 1970), p. 134.
- [15] A. G. Redfield, *Phys. Rev.* **98**, 1787 (1955); K. Tomita, *Prog. Theor. Phys.* **19**, 541 (1958).
- [16] L. Q. Lambert, *Phys. Rev. B* **7**, 1834 (1973); R. Boscaino, M. Brai, and I. Ciccarello, *ibid.* **13**, 2798 (1976).
- [17] R. Boscaino, F. M. Gelardi, and R. N. Mantegna, *Phys. Lett. A* **103**, 391 (1984); in *Structure and Dynamics of Molecular Systems*, edited by R. Daudel *et al.* (Reidel, Dordrecht, 1985), p. 149.